Synthetic S-2 and H-5 Segments of the Shaker K^+ Channel: Secondary Structure, Membrane Interaction, and Assembly within Phospholipid Membranes†

Hadas Peled and Yechiel Shai*

Department of Membrane Research and Biophysics, Weizmann Institute of Science, Rehovot, 76100 Israel

Received September 14, 1993; Revised Manuscript Received April 11, 1994®

ABSTRACT: Current models of voltage-activated K^+ channels predict that the channels are formed by the coassembly of four polypeptide monomers, each of which consists of six transmembrane segments (S1–S6) and long terminal domains. The aqueous pores are thought to be composed of the conserved H-5 regions contributed by four monomers. In this study, two putative membrane-embedded segments of the Shaker K^+ channel were synthesized. One segment corresponds to the putative, transmembrane helix S-2 (amino acids 275–300), and the other corresponds to the highly conserved 12 amino acid residues within the H-5 region [amino acids 432–443, designated (12)H-5)]. Structural and functional characterization at elevated lipid/peptide molar ratios (>3000:1) was performed on the two segments, as well as on a previously synthesized 21 amino acid long peptide with a sequence resemblimg the entire H-5 region (designated (21)H-5) (Peled & Shai, 1993). Circular dichroism spectroscopy revealed that S-2 adopts predominantly α-helical structure in both trifluoroethanol and 35 mM SDS (78% or 99%, respectively), while (12)H-5 and (21)H-5 adopt low α-helical structure only in the presence of 35 mM SDS. Functional characterization demonstrated that S-2 and (12)H-5 segments bind to zwitterionic phospholipids, with partition coefficients on the order of 10^4 M^{-1}. Resonance energy transfer measurements, between donor/acceptor-labeled pairs of peptides, revealed that the peptides self-associate in their membrane-bound state, which may correlate with the existence of functional interactions between the conserved (12)H-5 regions of different subunits of K^+ channels (Kirsch et al., 1993). Furthermore, membrane-bound (12)H-5 or (21)H-5 associates with membrane-bound S-2, but does not associate with unrelated, membrane-bound α-helical peptides. These results demonstrate molecular recognition between transmembrane segments of the Shaker K^+ channel that might contribute to the oligomerization and correct assembly of the monomers, which result in the formation of a functional channel.

Ion channels are integral membrane proteins that allow the passage of specific ions through the phospholipid membrane barrier, which is an essential step for many cellular processes (Hille, 1992). Voltage-activated K^+ channels are a large and diverse group within the family of voltage-activated ion-conducting channels. These K^+ channels are assumed to be formed by the assembly of four polypeptide monomers of about 70 kDa each (Catterall, 1988; MacKinnon, 1991; Liman et al., 1992). Although crystallographic data are not yet available, the monomers are thought to be organized in well-defined structures within the cell membrane. Hydropathic analysis of the K^+ channel monomers suggests that they consist of six putative transmembrane segments (S1–S6) and an S5–S6 linker (termed the H-5 region), proposed to line the lumen of the channel. The monomers also contain long N- and C-terminal domains (Catterall, 1988). Both protein/lipid and protein/protein interactions are thought to determine the correct assembly of the channel. However, the structural components involved in the assembly process are not yet clear. Li et al. (1992) have proposed that the N-terminal domains of the Shaker K^+ channel monomers and the core region, which include the transmembrane domains, are involved in mediating the appropriate assembly of the channels. The existence, within the core region, of sites for monomer recognition was also proposed by McCormack et al. (1990).

Combined molecular biology and electrophysiological approaches indicated that the H-5 segment of K^+ channels is involved in the formation of the ion-conducting pore, thus suggesting its location in the lumen of the channel (MacKinnon & Miller, 1989; MacKinnon & Yellen, 1990; MacKinnon et al., 1990; Yellen et al., 1991; Hartmann et al., 1991; Yool & Schwarz, 1991; Heginbotham & MacKinnon, 1992). Recently, we utilized a spectrofluorometric approach to demonstrate that synthetic peptides, corresponding to the H-5 segment of the Shaker K^+ channel, bind to phospholipid membranes and self-assemble therein (Peled & Shai, 1993). These observations support the hypotheses that H-5 is a membrane-embedded segment and that it might contribute to the appropriate assembly of the core region of K^+ channel monomers. However, there is no direct experimental information on the structure and membrane localization of other segments of K^+ channel monomers.

Herein, the synthesis, fluorescent labeling, and characterization of two segments within the Shaker K^+ channel are described. One segment has a sequence identical to the that of putative transmembrane helix S-2 (amino acids 275–300), and the other has a sequence corresponding to the highly conserved 12 amino acid residues (amino acids 432–443) of the H-5 segment [termed (12)H-5]. A previously synthesized, 21 amino acid long peptide [termed (21)H-5], with a sequence corresponding to the entire H-5 region, was also utilized (Peled & Shai, 1993). Circular dichroism (CD[1]) spectroscopy revealed that synthetic S-2, but not (12)H-5 or (21)H-5, adopts

† This research was supported in part by the Joseph Cohn Center for Biomembrane Research and by the Pearl Levine Foundation for Research in the Neurosciences at the Weizmann Institute of Science. Y.S. is an Incumbent of the Adolpho and Evelyn Blum Career Development Chair in Cancer Research.

* Author to whom correspondence should be addressed. Telephone: 972-8-342711. Fax: 972-8-344112.

® Abstract published in *Advance ACS Abstracts,* May 15, 1994.

0006-2960/94/0433-7211$04.50/0

a predominately α-helical structure in a hydrophobic environment. Both S-2 and (12)H-5 bound strongly to zwitterionic phospholipid small unilamellar vesicles (SUV). Resonance energy transfer measurements, between donor/acceptor-labeled pairs of peptides, revealed that the peptides self-associate in their membrane-bound state. Moreover, membrane-embedded H-5 [either the truncated, 12 amino acid residue segment or the entire 21 amino acid residue H-5 segment] associates with membrane-bound S-2, but not with unrelated, membrane-bound, α-helical peptides. These results demonstrate molecular recognition between membrane-embedded segments of the Shaker K^+ channel that might contribute to the oligomerization and correct assembly of the monomers to form a functional channel.

MATERIALS AND METHODS

Materials. BOC-amino acid PAM-resins were purchased from Applied Biosystems (Foster City, CA), and BOC-amino acids were obtained from Peninsula Laboratories (Belmont, CA). Other reagents for peptide synthesis included trifluoroacetic acid (TFA) (Sigma), *N,N*-diisopropylethylamine (DIEA) (Aldrich, distilled over ninhydrin), dicyclohexylcarbodiimide (DCC) (Fluka), 1-hydroxybenzotriazole (HOBT) (Pierce), methylene chloride, and dimethylformamide (DMF) (Bio-Lab). Egg phosphatidylcholine (PC) was purchased from Lipid Products (South Nutfield, U.K.). Cholesterol (extra pure) was supplied by Merck (Darmstadt, Germany) and recrystallized twice from ethanol. 5(and 6)-Carboxytetramethylrhodamine succinimidyl ester was obtained from Molecular Probes (Eugene, OR). NBD was obtained from Sigma. Sodium dodecyl sulfate (SDS) was purchased from BDH (Poole, England). All other reagents were of analytical grade. Buffers were prepared using double-glass-distilled water.

Peptide Synthesis and Fluorescent Labeling. The peptides were synthesized by the solid-phase method on amino acid-PAM-resins (0.075 mequiv) (Merrifield et al., 1982). At the end of the synthesis, the resin-bound peptides were treated for 3 min with 20% piperidine in DMF to remove the formyl protecting group from the tryptophan, cleaved from the resins by HF, and finally extracted with ether after HF evaporation. All of the peptides contained one major peak (as revealed by RP-HPLC), which was shown to be >70% pure peptide by weight. The H-5 peptides were purified by RP-HPLC on a C_4 reverse-phase Vydac column (300-Å pore size), and S-2 was purified on a CN reverse-phase DuPont column. The columns were eluted in 40 min at a flow rate of 0.6 mL/min, using a linear gradient of 25–80% acetonitrile in water in the presence of 0.1% TFA (v/v). The purified peptides were shown to be homogeneous (~99%) by analytical HPLC. The peptides were subjected to amino acid analysis in order to confirm their composition.

Labeling of the N-terminus of the peptides with fluorescent probes was achieved via the labeling of resin-bound peptides, as previously described (Rapaport & Shai, 1991, 1992). Resin-bound peptides (30–40 mg, 10–25 μmol) were treated with TFA (50% (v/v) in methylene chloride) to remove the BOC protecting group from the N-terminal amino group of the attached peptides. The resin-bound peptides were then reacted with either (i) 5 (and 6)-carboxytetramethylrhodamine succinimidyl ester (Rho-Suc) (3–4 equiv) in dry DMF containing 2.5% (v/v) diisopropylethylamine or (ii) 4-fluoro-7-nitrobenz-2-oxa-1,3-diazole (NBD-F) in dry DMF. These two reactions led to the formation of resin-bound N^1-Rho-peptides or N^1-NBD-peptides, respectively. After 48 h, the mixtures were washed thoroughly with methylene chloride. The peptides were then cleaved from the resins by HF and purified by reverse-phase HPLC, as described above.

Preparation of Small Unilamellar Vesicles. Small unilamellar vesicles (SUV) were prepared by the sonication of egg phosphatidylcholine (PC) as previously described (Shai et al., 1990). Briefly, dry lipid and cholesterol (10:1, w/w) were dissolved in a $CHCl_3$/MeOH mixture (2:1, v/v). The solvents were then evaporated under a stream of nitrogen, and the lipids (at a concentration of 7.2 mg/mL) were put under vacuum for 1 h and then resuspended in the appropriate buffer via vortex mixing. The resultant lipid dispersion was then sonicated for 10–30 min in a bath-type sonicator (G1125SP1 sonicator, Laboratory Supplies Company Inc., Hicksville, NY) until clear. The lipid concentration of the supernatant was determined by phosphorus analysis (Bartlett et al., 1959). Vesicles were visualized using a JEOL JEM 100B electron microscope (Japan Electron Optics Laboratory Co., Tokyo, Japan). Vesicles prepared in this fashion are unilamellar, with an average diameter of 20–50 nm (Papahadjopoulos & Miller, 1967).

CD Spectroscopy. CD spectra were measured at room temperature using a Jasco J-500A spectropolarimeter after the instrument was calibrated with (+)-10-camphorsulfonic acid. A cylindrical fused quartz optical cell of 0.5 mm path length was used. Spectra were obtained at wavelengths of 195–250 nm. Seven scans were taken at a scan rate of 20 nm/min. The peptides were scanned in either 40% trifluoroethanol (TFE) or 35 mM SDS in buffer (16.7 mM NaCl and 4.2 mM HEPES/SO_4^{2-}, pH 7.3). The peptides were scanned at concentrations of (0.8–3.0) $\times 10^{-5}$ M. Fractional helicities (Wu et al., 1981) were calculated as follows:

$$f_h = \frac{([\theta]_{222} - [\theta]^0_{222})}{[\theta]^{100}_{222}}$$

where $[\theta]_{222}$ is the experimentally observed mean residue ellipticity at 222 nm, and values for $[\theta]^0_{222}$ and $[\theta]^{100}_{222}$, corresponding to 0% and 100% helix content at 222 nm, were estimated at 2000 and 30 000 deg·cm^2/dmol, respectively (Chen et al., 1974; Wu et al., 1981).

Fluorescence Measurements. (a) Intrinsic Tryptophan Fluorescence. Changes in the intrinsic tryptophan fluorescence were measured in buffer and upon binding to PC SUV vesicles. Peptides were added separately to quartz cuvettes, each containing 400 μL buffer (50 mM Na_2SO_4 and 25 mM HEPES/SO_4^{2-}, pH 6.8), such that the final concentrations of the peptides were 1 μM for (12)H-5 and (21)H-5 and 5.6 and 2.8 μM for S-2 in buffer and in the presence of vesicles, respectively. Spectra were taken in buffer or in the presence of 1000 μM PC SUV. Lower concentrations were utilized for the H-5-derived peptides due to the presence of two consecutive tryptophan residues within their sequence. Emission spectra were measured using an SLM Aminco 8000 spectrofluorometer, with the excitation monochromator set at 280 nm using a 4-nm slit. Fluorescence readings were corrected for vesicle light scattering.

(b) NBD Fluorescence Measurements. Changes in the fluorescence of NBD-labeled peptides were measured upon

[1] Abbreviations: BOC, butyloxycarbonyl; CD, circular dichroism; DCC, dicyclohexylcarbodiimide DIEA, diisopropylethylamine; DMF, dimethyl formamide; Flu, fluorescein; HF, hydrogen fluoride; HOBT, 1-hydroxybenzotriazole; NBD, 7-nitrobenz-2-oxa-1,3-diazol-4-yl; Pam, (phenylacetamido)methyl; PC, egg phosphatidylcholine; Rho, tetramethylrhodamine; RP-HPLC, reverse-phase high-performance liquid chromatography; SDS, sodium dodecyl sulfate; SUV, small unilamellar vesicles; TFA, trifluoroacetic acid; TFE, trifluoroethanol.

binding to PC vesicles. NBD-labeled peptide (0.1 μM) was added to 400 μL buffer (50 mM Na_2SO_4 and 25 mM HEPES/SO_4^{2-}, pH 6.8) containing 300 μM PC SUV to establish a lipid/peptide molar ratio for which most of the peptide is bound to lipid. Emission spectra were measured using a Perkin-Elmer LS-50B spectrofluorometer with excitation set at 467 nm, using a 5-nm slit.

Binding Experiments. The environment-sensitive NBD fluorophore has been utilized previously for polarity and binding studies (Kenner & Aboderin, 1971; Frey & Tamm, 1990; Rapaport & Shai, 1991; Pouny & Shai, 1992; Ben-Efraim et al., 1993). Briefly, PC SUV were added successively to 0.1 μM NBD-labeled peptides at 24 °C. Fluorescence intensities were measured as a function of the lipid/peptide molar ratio on a Perkin-Elmer LS-50B spectrofluorometer, with excitation set at 467 nm (using a 10-nm slit) and emission set at 530 nm (using a 5-nm slit) in three separate experiments. To determine the extent of the lipids' contribution to any given signal, the readings observed when unlabeled peptides were titrated with lipid vesicles were subtracted as background from the recorded fluorescence intensities. The binding isotherms were analyzed as a partition equilibrium (Schwarz et al., 1986, 1987; Rizzo et al., 1987; Beschiaschvili & Seelig, 1990; Rapaport & Shai, 1991), using the following formula:

$$X_b^* = K_p^* C_f$$

where X_b^* is defined as the molar ratio of bound peptide per 60% of the total lipid, assuming that the peptides were initially partitioned only over the outer leaflet of the SUV, as had been suggested previously (Beschiaschvili & Seelig, 1990). K_p^* corresponds to the partition coefficient, while C_f represents the equilibrium concentration of free peptide in the solution. To calculate X_b, F_∞ (the fluorescence signal obtained when all of the peptide is bound to lipid) was extrapolated from a double-reciprocal plot of F (total peptide fluorescence) versus C_L (total concentration of lipids) (Schwarz et al., 1986). Since the fluorescence intensities of unbound peptide, F_0, as well as bound peptide, F, were known, the fraction of membrane-bound peptide, f_b, could be calculated using the following formula:

$$f_b = (F - F_0)/(F_\infty - F_0)$$

Once the value of f_b has been calculated, it is then possible to calculate C_f, as well as the extent of peptide binding, X_b^*. The curves resulting from plotting X_b^* versus free peptide, C_f, are referred to as the conventional binding isotherms.

Resonance Energy Transfer Measurements. Resonance energy transfer experiments (RET) were conducted as previously described (Rapaport & Shai, 1992; Gazit & Shai, 1993b). Fluorescence spectra were obtained at room temperature on an LS-50B spectrofluorometer, with the excitation monochromator set at 450 nm with a 5-nm slit width. Measurements were performed in a 0.5-cm path length glass cuvette in a final reaction volume of 0.4 mL. Although the excitation maximum for NBD is 467 nm, a lower wavelength was chosen in order to minimize the excitation of tetramethylrhodamine (Harris et al., 1991).

The efficiency of energy transfer (E) was determined by the decrease in the quantum yield of the donor as a result of the addition of acceptor. E was determined experimentally from the ratio of the fluorescence intensities of the donor in the presence (I_{da}) and in the absence (I_d) of the acceptor at the emission wavelength of the donor, after correcting for membrane light scattering and the contribution of the emission of the acceptor. The percentage value of E is given in following equation:

$$E = (1 - I_{da}/I_d)100$$

The correction for light scattering was made by subtracting the signal obtained when unlabeled analogues at concentrations that are equal to the sum of the donor and the acceptor were added to vesicles. Correction for the contribution of acceptor emission was made by subtracting the signal produced by the acceptor-labeled analogue alone.

RESULTS

To investigate the possible involvement of putative membrane-embedded segments from the core region of the Shaker K^+ channel in the channel's assembly, two peptides were synthesized by a solid-phase method. One, which contains 26 amino acids, has a sequence identical to the putative α-helical S-2 region of the Shaker K^+ channel (amino acids 275–300), and the other has a sequence corresponding to the 12 highly conserved amino acids from the H-5 region (amino acids 432–443). A previously synthesized, 21 amino acid long peptide, with a sequence corresponding to the entire H-5 region (Peled & Shai, 1993), was also utilized. Each peptide was labeled selectively at its N-terminal amino acid with either the fluorophore NBD (to serve as an environment-sensitive probe and as an energy donor) or tetramethylrhodamine (Rho, to serve as an energy acceptor). The sequences of the peptides, their fluorescent derivatives, and their designations, as well as those of other fluorescently labeled peptides utilized in this study, are shown in Table 1. The secondary structure of the peptides was determined by CD spectroscopy. Furthermore, their abilities to bind to zwitterionic phospholipid membranes, to self-associate, and to form heteroaggregates in their membrane-bound states were determined.

Secondary Structure Determination Using CD Spectroscopy. The secondary structures of (12)H-5, (21)H-5, and S-2 in a hydrophobic environment was estimated from their CD spectra in 40% TFE and in the membrane mimetic environment of sodium dodecyl sulfate (SDS) micelles (Figure 1). Due to the low solubility of the peptides in buffer, their incorporation into vesicles at the relatively high peptide/lipid molar ratios required for CD measurements was unsuccessful. S-2 exhibited mean residual ellipticities $[\theta]_{222}$ of −25 400 and −31 700 deg·cm²/dmol in 40% TFE and in 35 mM SDS, respectively. These values correspond to very high fractional helicities of 78% and 99% in the TFE and SDS solutions, respectively (Wu et al., 1981). This high α-helical content supports theoretical models proposing S-2 as one of the transmembrane α-helices building the core region of the channel. No significant CD signal was obtained with (12)H-5 or with (21)H-5 in 40% TFE in water. However, in the presence of 35 mM SDS, (12)H-5 and (21)H-5 exhibited low mean residual ellipticities $[\theta]_{222}$ of −6300 and −8500 deg·cm²/dmol, respectively. These values correspond to relatively low fractional helicities of ~15% and ~20%, respectively (Figure 1).

NBD Fluorescence Studies and Binding Experiments. The sensitivity of the NBD group to the dielectric constant of its environment facilitates its utilization for polarity and binding studies (Kenner & Aboderin, 1971; Frey & Tamm, 1990; Baidin & Huang, 1990; Rapaport & Shai, 1991; Pouny & Shai, 1992; Ben-Efraim & Shai, 1993). In this study, the fluorescence emission spectra of NBD-labeled S-2, (12)H-5, and (21)H-5 [see Peled and Shai (1993)] and the spectrum of NBD-aminoethanol, which served as a control, were measured either in aqueous solutions or in the presence of PC vesicles. A profile of the fluorescence intensity and maximum emission wavelength of NBD-S-2 in buffer and the profiles

Table 1: Sequences and Designations of the Peptides Investigated

peptide no.	peptide designation	peptide modification	peptide sequence
1	(12)H-5	X = H	
2	NBD-(12)H-5	X = NBD	X-NH-AFWWAVVTMTTV
3	Rho-(12)H-5	X = Rho	
4	(21)H-5	X = H	
5	NBD-(21)H-5	X = NBD	X-NH-AFWWAVVTMTTVGYGDMTPVG
6	Rho-(21)H-5	X = Rho	
7	S-2	X = H	
8	NBD-S-2	X = NBD	X-NH-ITDPFFLIETLCIIWFTFELTVRFLA
9	Rho-S-2	X = Rho	
10	Rho-pardaxin[a]	X = Rho	X-NH-GFFALIPKIISSPLFKTLLSAVGSALSSSGGQE
11	Rho-cecropin[b]	X = Rho	X-NH-RWKIFKKIEKMGRNIRDGIVKAGPAIEVLGSAKAI

[a] Taken from Rapaport and Shai (1992). [b] Taken from Gazit and Shai (unpublished results).

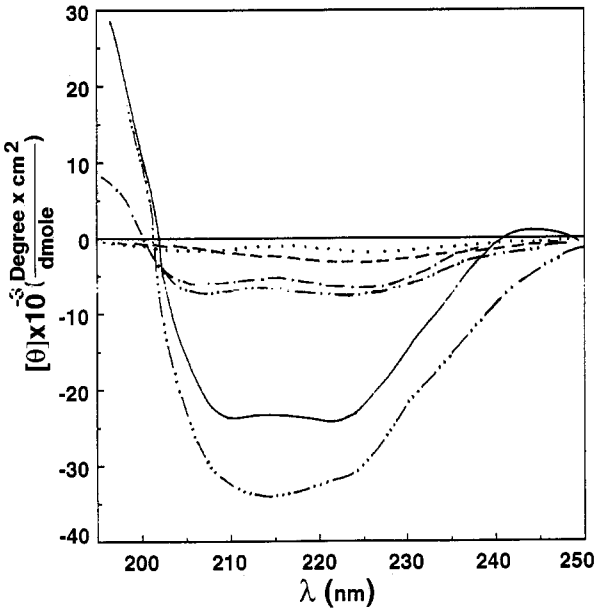

FIGURE 1: CD spectra of the synthetic peptides. Spectra were taken as described in the Materials and Methods section at peptide concentrations of 0.8×10^{-5} to 3.0×10^{-5} M: (12)H-5 in 40% TFE (···); (12)H-5 in 1% SDS (-·-·); (21)H-5 in 40% TFE (- - -); (21)H-5 in 1% SDS (-·····); S-2 in 40% TFE (—); S-2 in 1% SDS (-·-·-·-).

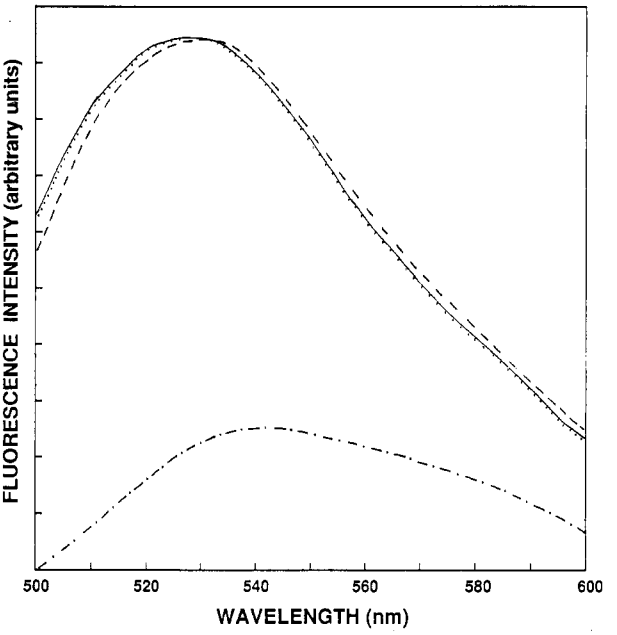

FIGURE 2: Fluorescence emission spectra of NBD-labeled peptides. Spectra were determined in the presence or absence of PC SUV (300 μM phospholipids) in buffer composed of 50 mM Na_2SO_4 and 25 mM HEPES/SO_4^{2-} (pH 6.8). The excitation wavelength was set at 467 nm, and emission was scanned from 500 to 600 nm: 0.1 μM NBD-(12)H-5 in the presence of vesicles (—); 0.1 μM NBD-(21)H-5 in the presence of vesicles (···); 0.1 μM NBD-S-2 in the presence of vesicles (- - -); 1 μM NBD-S-2 in buffer (-·-·).

of all of the NBD-labeled peptides in the presence of PC SUV are shown in Figure 2. The concentration of NBD-S-2 in buffer was 10-fold higher than its concentration in the presence of vesicles. Similar results were obtained with NBD-(12)H-5 and NBD-(21)H-5. When NBD-S-2, NBD-(12)H-5, or NBD-(21)H-5 was placed in buffer, the peptides exhibited emission maxima around 540 nm and a low quantum yield in their fluorescence intensities (Figure 2), similar to previously reported emission wavelength maxima for NBD derivatives placed in hydrophilic environments (Rajarathnam et al., 1989; Rapaport & Shai, 1991; Pouny & Shai, 1992). However, when added to solutions of PC vesicles (pH 6.8), the NBD-labeled peptides, but not NBD-aminoethanol, exhibited enhanced increases in their fluorescence intensities and blue shifts in their fluorescence emission maxima [λ_{max} = 528 ± 1 nm for NBD-S-2 and λ_{max} = 526 ± 1 nm for NBD-(12)H-5 and NBD-(21)H-5 (Figure 2)]. These changes reflect the relocation of the NBD groups into more hydrophobic environments. In these experiments, the lipid/peptide molar ratio was consistently maintained at an elevated level (3000:1), so that the spectral contributions of free peptide would be negligible.

To determine the surface partition coefficients, with phospholipid membranes, of the synthesized peptides, samples of NBD-labeled peptides were mixed with increasing amounts of PC SUV at pH 6.8. The zwitterionic PC was used to avoid contributions of phospholipid head group charges to binding processes. To generate binding curves, increases in the fluorescence intensities of the NBD-labeled peptides were plotted as a function of the lipid/peptide molar ratios (see trace A in Figures 3–5 for NBD-(12)H-5, NBD-(21)H-5, and NBD-S-2, respectively). Since the concentrations of the NBD-labeled peptides in the mixtures were low, the peptides were assumed not to disrupt the bilayer structure. When unlabeled peptides were titrated with lipids up to the maximal concentrations used with NBD-labeled peptides, the fluorescence intensities of these solutions, after subtraction of the contribution of the vesicles, remained unchanged.

The binding isotherms were analyzed as partition equilibriums, as described in the Materials and Methods section. The curves obtained by plotting X_b* (the molar ratio of bound peptide per 60% of the total lipid assumed to be in the outer leaflet) versus C_f (the equilibrium concentration of free peptide in the solution), referred to as the conventional binding isotherms, are shown as trace B in Figures 3–5 for NBD-(12)H-5, NBD-(21)H-5, and NBD-S-2, respectively. The surface partition coefficients, K_p*, were estimated by extrapolating the initial slopes of the curves to zero C_f values. The K_p* values are $(1.0 \pm 0.2) \times 10^4$, $(3.0 \pm 0.5) \times 10^4$, and

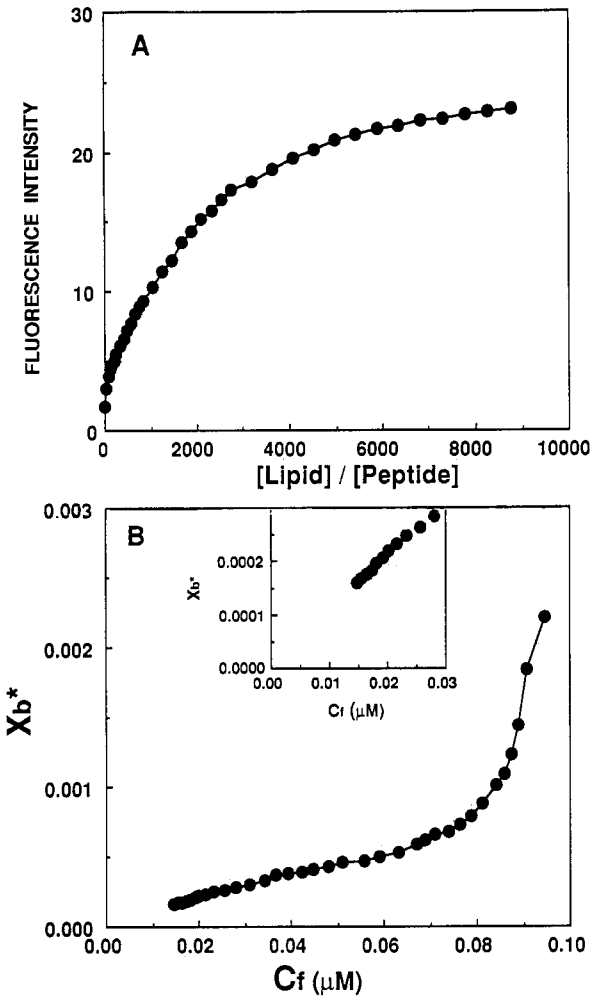

FIGURE 3: Increases in the fluorescence of NBD-(12)H-5 upon titration with PC vesicles (A) and the resulting binding isotherm (B). NBD-(12)H-5 (0.1 μM) was titrated with PC SUV, with excitation set at 467 nm and emission recorded at 530 nm. The experiment was performed at room temperature in buffer composed of 50 mM Na_2SO_4 and 25 mM HEPES/SO_4^{2-} (pH 6.8). The Binding isotherm was derived from A by plotting X_b* (molar ratio of bound peptide per 60% lipid) versus C_f (equilibrium concentration of free peptide in the solution). The inset shows the low concentration range of the main figure.

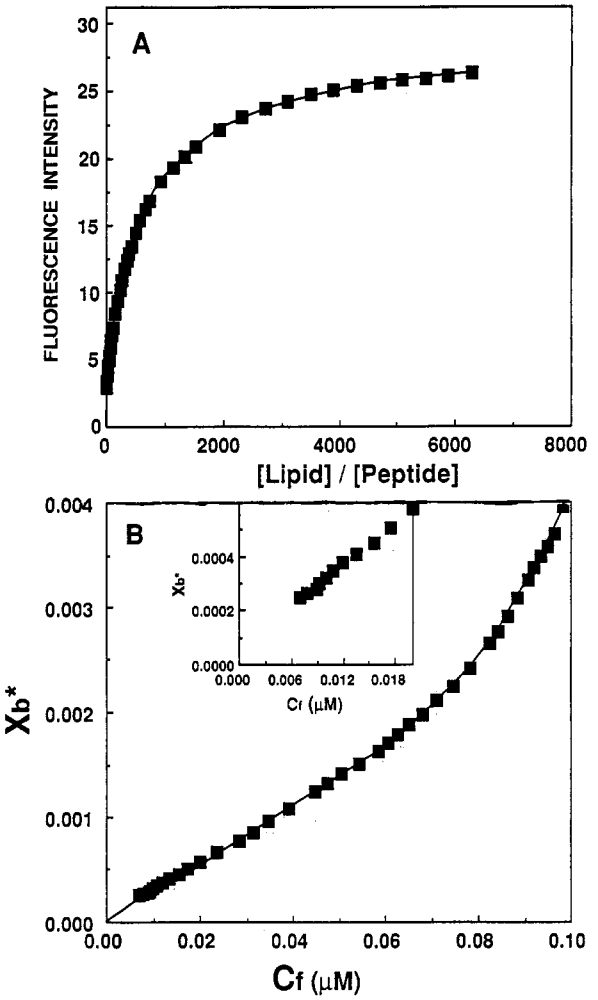

FIGURE 4: Increases in the fluorescence of NBD-(21)H-5 upon titration with PC SUV (A) and the resulting binding isotherm (B). NBD-(21)H-5 (0.1 μM) was titrated with PC vesicles, with excitation set at 467 nm and emission recorded at 530 nm. The binding isotherm was derived from A as described in the legend of Figure 3.

(4.2 ± 0.4) × 10^4 M^{-1} for (12)H-5, (21)H-5, and S-2, respectively. These K_p* values are within the range of those obtained for membrane-permeating bioactive peptides, such as melittin and its derivatives (Stankowski & Schwarz, 1990), the *Staphylococcus* δ-toxin (Thiaudiére et al., 1991), the antibiotic dermaseptin (Pouny et al., 1992), and pardaxin and its analogues (Rapaport & Shai, 1991).

Tryptophan Fluorescence Studies. The NBD fluorescence facilitates studies at a very low concentration of labeled peptide (>10-fold less than that utilized in tryptophan fluorescence studies) and at a very high lipid/peptide molar ratio (>3000:1). These conditions are prerequisite to investigate the initial steps involved in the interaction of the peptides with membranes. However, since the NBD moiety is attached specifically to the N-terminal ends of the peptides, the NBD fluorescence studies facilitate the determination of the location of the N-terminals of the peptides in a membrane-bound state. To determine the environments of other parts of the peptides in their membrane-bound state, the intrinsic fluorescence of the tryptophan was used. Similarly to NBD, the fluorescence of tryptophan is sensitive to the surroundings, such that the movement of tryptophan from an aqueous to a lipid environment is accompanied by an increase in the fluorescence intensity and a blue shift of the fluorescence emission maximum (Lakowicz, 1983; Surewicz & Epand, 1984; McKnight et al., 1991; Chung et al., 1992). (12)H-5 and (21)H-5 [taken from Peled and Shai (1993)] have two consecutive tryptophan residues near their N-terminals, while S-2 has a single tryptophan residue located in the middle of the hydrophobic face of the helical peptide, as revealed by the Schiffer and Edmondson (1967) wheel projection (Figure 9). The fluorescence emission spectra of (12)H-5, (21)H-5, and S-2 were measured either in aqueous solutions or in the presence of PC vesicles (Figure 6). When placed in buffer, (12)H-5 and (21)H-5 exhibited emission maxima of λ_{max} = 355 ± 1 and 359 ± 1 nm, respectively, indicating that the tryptophans are exposed to a hydrophilic environment (Figure 6A,B). S-2 exhibited a lower emission maximum of 344 ± 2 nm, which reveals a less hydrophilic environment for the tryptophan. However, upon the addition of the three peptides separately to solutions of 1000 μM PC vesicles (pH 6.8), the peptides exhibited enhanced increases in their fluorescence intensities and blue shifts in their fluorescence emission maxima (λ_{max} = 340 ± 2, 332 ± 2, and 331 ± 2 nm for (12)H-5, (21)H-5, and S-2, respectively).

These changes reflect the relocation of the tryptophan residues into a more hydrophobic environment. These results are qualitatively similar to those obtained in the NBD fluorescence studies, suggesting that, in addition to the N-terminal amino acids of the three segments, the N parts of both (12)H-5 and (21)H-5, and the middle part of S-2 are embedded within the membrane. This result correlates with

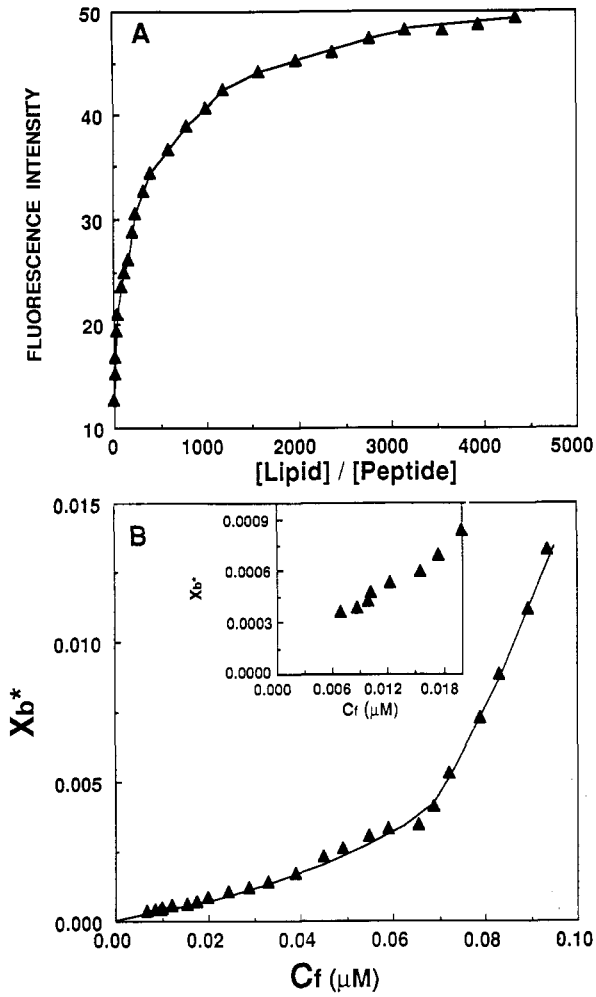

FIGURE 5: Increases in the fluorescence of NBD-S-2 upon titration with PC SUV (A) and the resulting binding isotherm (B). NBD-S-2 (0.1 μM) was titrated with PC vesicles, with excitation set at 467 nm and emission recorded at 530 nm. The binding isotherm was derived from A as described in the legend of Figure 3.

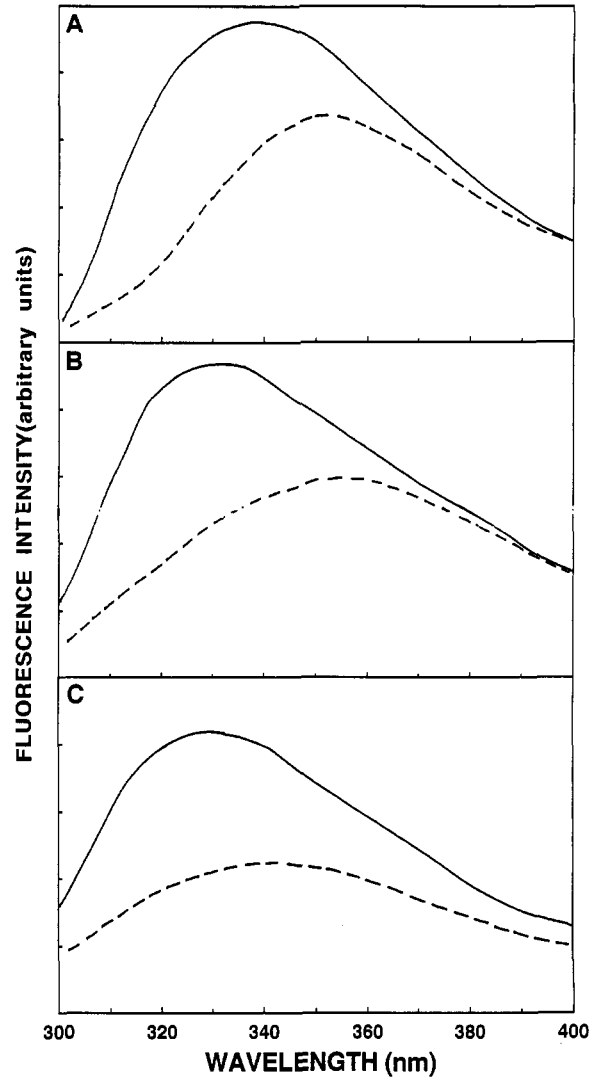

FIGURE 6: Fluorescence emission spectra of tryptophan. Spectra were determined in the presence or absence of PC SUV (1000 μM phospholipids) in buffer composed of 50 mM Na_2SO_4 and 25 mM HEPES/SO_4^{2-} (pH 6.8). The excitation wavelength was set at 280 nm, and emission was scanned from 300 to 400 nm: (A) (12)H-5; (B) (21)H-5; (C) S-2. Symbols: in buffer (- - -); in the presence of vesicles (—).

the prediction that S-2 is a transmembrane helix (Guy & Conti, 1990). That the maximum emission wavelength of (12)H-5 (340 ± 2 nm) is significantly higher than that of (21)H-5 (332 ± 2 nm) in the presence of vesicles may be attributed to the larger contribution of the unbound fraction of (12)H-5 to the observed signal. This explanation may be supported by the fact that, at the relatively high concentrations of the peptides used (1–2.8 μM, as compared with 0.1 μM in the NBD fluorescence studies), and at 1000 μM phospholipid vesicles, significant amounts of peptides are not bound, and hence the signal of unbound peptide contributes to the total signal. This effect is more profound with (12)H-5, which has a lower partition coefficient than (21)H-5 [$(1.0 \pm 0.2) \times 10^4$ and $(3.0 \pm 0.5) \times 10^4$ M^{-1}, respectively]. The situation is different in the cases of NBD-(12)H-5 and NBD-(21)H-5, where their emission maxima were measured near the saturation condition (lipid/peptide molar ratios >3000:1), and therefore, identical emission maxima were obtained. The relatively hydrophobic surroundings for tryptophan when S-2 is placed in buffer may be in part due to the formation of peptide aggregates of this hydrophobic peptide at the relatively high concentration of peptide employed (5.6 μM).

Resonance Energy Transfer (RET) Experiments. The ability of (21)H-5 to associate with the membrane-bound N-terminal extended form of the H-5 region has been shown previously (Peled & Shai, 1993). Herein, whether (12)H-5, (21)H-5, or S-2 can self-associate or form heteroaggregates within the membranes at low peptide/lipid molar ratios was examined. For this, NBD-labeled peptides, selectively labeled at their N-terminal amino acids, were used as energy donors, and Rho-labeled peptides were used as energy acceptors (Table 1). RET measurements were performed as described in the Materials and Methods section. Examples of typical profiles of the energy transfer from NBD-(12)H-5 to Rho-(12)H-5, in the presence of PC phospholipid vesicles, are depicted in Figure 7A, and those showing the energy transfer from NBD-(12)H-5 to Rho-pardaxin, in the presence of PC phospholipid vesicles, are depicted in Figure 7B. The addition of Rho-(12)H-5 (final concentrations of 0.025–0.1 μM) to NBD-(12)H-5 (0.04 μM) with PC phospholipid vesicles (100 μM) significantly quenched the donor's emission and increased the acceptor's emission, which is consistent with energy transfer. Similar experiments were performed using mixtures of NBD- and Rho-labeled (12)H-5, (21)H-5, S-2, pardaxin, or cecropin B as donors and acceptors in various combinations.

To determine the actual percentage of energy transfer, the amounts of lipid-bound acceptors (Rho-peptides, termed "bound acceptor") at the various acceptor-peptide concentrations were calculated from the binding isotherms of the corresponding NBD-labeled peptides as previously described (Pouny et al., 1992). The curves of the experimentally derived

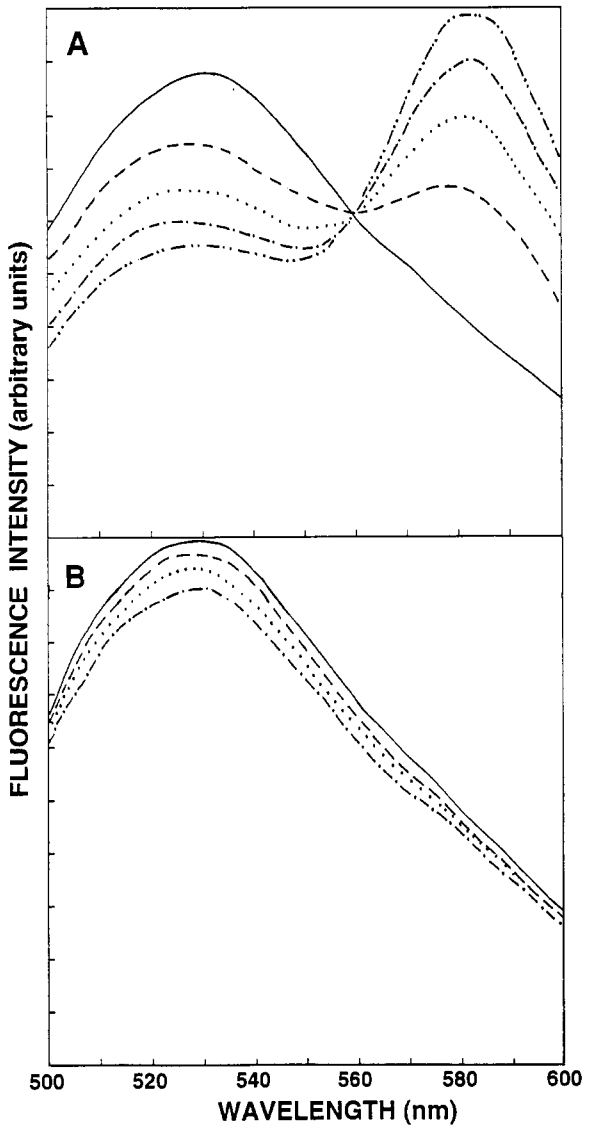

FIGURE 7: Fluorescence energy transfer dependence on Rho-peptide (acceptor) concentration. The spectrum of NBD-(12)H-5 (0.04 μM), the donor peptide, was recorded in the presence or absence of various concentrations of the acceptor peptide Rho-(12)H-5 or Rho-pardaxin. Each spectrum was recorded in the presence of PC vesicles (100 μM phospholipids) in buffer composed of 50 mM Na_2SO_4 and 25 mM HEPES/SO_4^{2-} (pH 6.8). The excitation wavelength was set at 450 nm; emission spectra were recorded from 500 to 600 nm. Panel A: (—) 0.04 μM NBD-(12)H-5; (- - -) a mixture of 0.04 μM NBD-(12)H-5 and 0.025 μM Rho-(12)H-5; (···) a mixture of 0.04 μM NBD-(12)H-5 and 0.05 μM Rho-(12)H-5; (-·-·) 0.04 μM NBD-(12)H-5 and 0.075 μM Rho-(12)H-5; (-·····) 0.04 μM NBD-(12)H-5 and 0.10 μM Rho-(12)H-5. Panel B: (—) 0.04 μM NBD-(12)H-5; (- - -) a mixture of 0.04 μM NBD-(12)H-5 and 0.025 μM Rho-pardaxin; (···) a mixture of 0.04 μM NBD-(12)H-5 and 0.05 μM Rho-pardaxin; (-·-·) 0.04 μM NBD-(12)H-5 and 0.10 μM Rho-pardaxin.

percentages of energy transfer versus the bound acceptor/lipid molar ratios are depicted in Figure 8. A curve corresponding to a random distribution of monomers (Fung & Stryer, 1978), assuming an R_0 of 51 Å, which was previously calculated for the NBD/Rho donor/acceptor pair (Gazit & Shai, 1993b), is also depicted. A high percentage of energy transfer was obtained with NBD-(12)H-5/Rho-(12)H-5, NBD-(21)H-5/Rho-(21)H-5, NBD-S-2/Rho-S-2, NBD-S-2/Rho-(12)H-5, and NBD-S-2/Rho-(21)H-5 pairs (Figure 8). These values are markedly higher than those that would be obtained if the distribution of monomers was assumed to be random. However, the efficiencies of energy transfer between either NBD-(12)H-5 or NBD-(21)H-5, when serving as donors, and the unrelated membrane-interacting peptides,

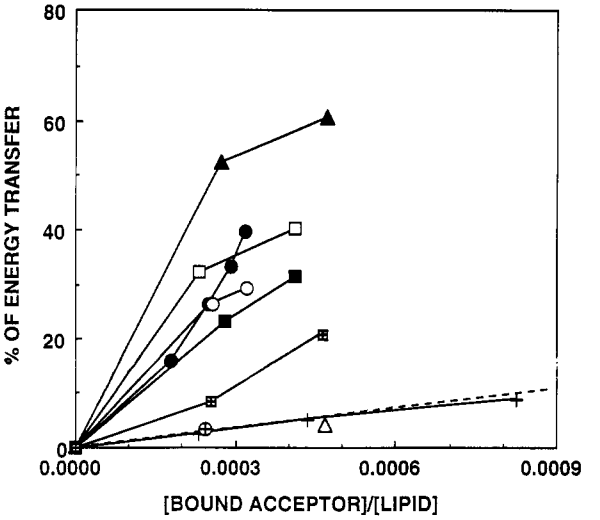

FIGURE 8: Theoretically and experimentally derived percentages of energy transfer versus bound acceptor/lipid molar ratio. The amounts of lipid-bound acceptor (Rho-peptides), C_b, at various acceptor concentrations were calculated from the binding isotherms. First, the fractions of bound acceptor, f_b, were calculated for the various peptide/lipid molar ratios from their binding isotherms (see Figures 3–5) and were then used to calculate the amount of bound acceptor (Pouny et al., 1992). Symbols: filled circles, NBD-(12)H-5/Rho-(12)H-5; filled triangles, NBD-S-2/Rho-S-2; filled squares, NBD-(21)H-5/Rho-(21)H-5; open circles, NBD-S-2/Rho-(12)H-5; open squares, NBD-S-2/Rho-(21)H-5; crosses, NBD-(12)H-5/Rho-pardaxin; crossed squares, NBD-S-2/Rho-cecropin; open triangles, NBD-(12)H-5/Rho-cecropin; crossed circles, NBD-S-2/Rho-pardaxin; dashed line, random distribution of the monomers (Fung & Stryer, 1978), assuming an R_0 of 51 Å.

Rho-cecropin and Rho-pardaxin, resemble those observed for random distribution, as does the efficiency of energy transfer for the NBD-S-2/Rho-pardaxin couple (Figure 8).

Thus, (12)H-5, (21)H-5, and S-2 appear to associate rather than distribute randomly throughout the phospholipid membranes. These results demonstrate that the predominantly non-α-helical H-5-derived segments can form heteroaggregates with α-helical S-2 segments in their membrane-bound state. The α-helices of the NBD-S-2/Rho-cecropin B pair showed significant energy transfer, although lower than in the other cases. The association of these two α-helices might be explained in terms of charge attraction and will be elaborated in the Discussion section.

DISCUSSION

Recognition and interaction sites between the subunits of membranal proteins were shown to exist in several cases. Such sites exist in (i) the intracellular domains of potassium channels (Li et al., 1992; Shen et al., 1993), (ii) the extracellular domains of the acetylcholine receptor subunits (Verrall & Hall, 1992; Yu & Hall, 1991), the platelet integrin GPIIb/IIIa (Frachet et al., 1992), and the Na^+, K^+-ATPase α-subunit (Lemas et al., 1992), and (iii) the transmembrane domains of integral membrane proteins, such as glycophorin A (Bormann et al., 1989; Lemmon et al., 1992), the bacteriorhodopsin (Kahn & Engelman, 1992), the T-cell receptor complex (Bonifacino et al., 1990a,b; Manolios et al., 1990), the tyrosine kinase receptor family (Sternberg & Gullick, 1990), the aspartate sensory receptor of *Escherichia coli* (Lynch & Koshland, 1991), and the lactose permease of *Escherichia coli* (Sahin-Toth et al., 1992).

The assembly of subunits of membranal proteins is thought to require a combination of interactions of different domains in these subunits. When such interactions were observed between the transmembrane segments of membrane proteins,

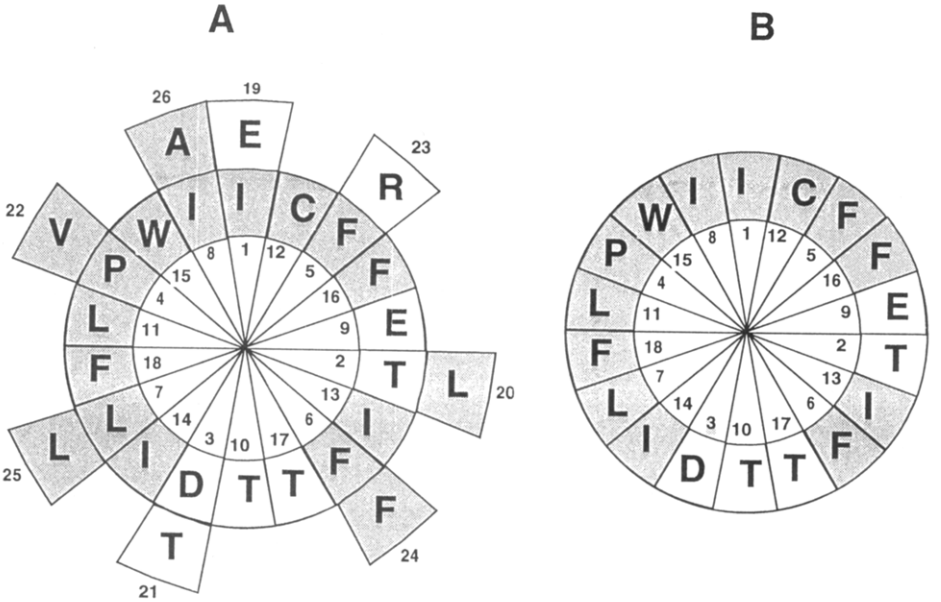

FIGURE 9: Schiffer–Edmundson wheel projections of the S-2 helix of the Shaker K^+ channel: (A) projection of amino acids 275–300; (B) projection of amino acids 275–292. Number 1 represents residue 275 of S-2. Shaded areas indicate hydrophobic amino acids.

highly hydrophobic α-helical segments were usually involved [see the review by Lemmon and Engelman (1992)]. Furthermore, self-assembly of membrane-embedded amphiphatic α-helices was also demonstrated with the shark repellent peptide neurotoxin, pardaxin (Rapaport & Shai, 1992), a model ion-channel forming peptide (Chung et al., 1992), and the α-5 helix of *Bacillus thuringiensis* δ-endotoxin (Gazit & Shai, 1993a). It should be indicated that although synthetic peptides corresponding to specific fragments of large proteins are not expected to mimic the precise function of their parent molecule, they may add significant structural information on those fragments. Moreover, although still limited, recent studies support a correlation between the structure and the organization of synthetic peptides, as compared to their parent molecule. Such studies were performed for both soluble [Dyson et al., 1992; Shin et al., 1993; see the review by Jaenicke (1991)] and membrane proteins [Kahn & Engelman, 1992; see the review by Lemmon and Engelman (1992)].

In the present study, it was demonstrated that synthetic segments from the Shaker K^+ channel can self-associate or form heteroaggregates in their membrane-bound state. The resonance energy transfer studies between donor- and acceptor-labeled peptides at extremely low acceptor/lipid molar ratios (Figure 8) demonstrated that the percentage of energy transfer between membrane-embedded monomers of H-5-derived segments, S-2 and H-5/S-2, is higher than that calculated for randomly distributed monomers. High energy transfer was already detected with all pairs at a peptide-acceptor/lipid molar ratio of $\sim$1:5000. If each SUV vesicle of 20–40-nm diameter (as determined by electron microscopy) is composed of 4000–10000 lipid molecules, and assuming that the peptides are equally distributed between the vesicles, then apparently as few as 2–3 molecules within one vesicle can associate. (21)H-5, the untruncated H-5 region, can self-assemble or coassemble with the α-helical S-2 segment to form heteroaggregates. Furthermore, even the short 12-mer segment, (12)H-5, which contains a highly conserved amino acid region of H-5, is sufficient to achieve self-assembly, assembly with the entire H-5 region, or coassembly with the α-helical S-2. These results show the existence of relatively specific interactions between membrane-embedded segments that do not have a tendency to form α-helical structures in a hydrophobic environment [(12)H-5 and (21)H-5] and a segment adopting a predominantly α-helical structure (S-2) (Figure 8). Although such interactions do not necessarily involve mainly or solely H-5 and S-2 in the native channel, they may be important in the oligomerization and the assembly of the protein. Whether H-5 can interact with other putative transmembrane segments derived from the Shaker potassium channel is now being investigated. Interestingly, the self-associating ability of the synthetic H-5 segments (Figure 8) correlates with the reported functionally important interactions between amino acids located in the conserved (12)H-5 regions of different subunits of K^+ channels (Kirsch et al., 1993).

The self-association of the H-5 segments and the ability of the segments to form heteroaggregates with S-2 in their membrane-bound state appear to be at least partially specific, since H-5 does not coassemble with every membrane-embedded peptide, e.g., the α-helices of pardaxin and cecropin (Figure 8). The energy transfer between the slightly amphipathic α-helix S-2 segment [as revealed by the Schiffer and Edmondson (1967) wheel projection, Figure 9] and the amphipathic α-helix of cecropin, although low, demonstrates an association between these unrelated α-helical peptides. Cecropin B is highly positively charged (net charge = +5), while NBD-S-2 is negatively charged (net charge = –3), with two of the negative charges on its hydrophilic face (Figure 9). Thus, the association between cecropin B and S-2 could be due to charge attraction, since they are oppositely charged. However, the self-association of S-2 segments and the association between S-2 and the H-5-derived segments occur, even though they are all negatively charged and expected to repel each other. Such repulsion was observed between membrane-bound amphiphilic α-helix monomers of the antibacterial peptide dermaseptin, which is positively charged and which was found to be randomly distributed in its membrane-bound state (Pouny et al., 1992). We suggest that the interactions dealt with in this paper do not necessarily have to be very specific, since under physiological conditions the probability of intra-subunit or inter-subunit interactions is much higher than the probability of a segment interacting with an unrelated protein. Furthermore, the formation of heteromultimeric potassium channels might require that inter-subunit interactions not be highly specific.

The structure of the pore formed by the H-5 segments is yet not clear, although various structural models have been

proposed. These include an α-helix, a long β-barrel, a short β-barrel, or a mixture of α-helix and β-barrel structures (Guy & Conti, 1990; Yellen et al., 1991; Hartmann et al., 1991; Yool & Schwarz, 1991; Durrel & Guy, 1992; Kirsch et al., 1992). The CD measurements (Figure 1) indicated a high α-helical content in the S-2 segment, as anticipated by a model of the K^+ channel (Durrel & Guy, 1992), but only low α-helix structure was observed with either the (21)H-5 or (12)H-5 segment. However, when an N-terminal-extended, 23 amino acid long H-5 is in a hydrophobic environment, CD measurements reveal significant α-helical content (Peled & Shai, 1993). These results support a model that proposes a partially α-helix structure at the N-terminal portion of H-5 (Guy & Conti, 1990).

In summary, it was demonstrated that synthetic segments resembling structurally different portions from the core region of the Shaker K^+ channel are preferentially self- or coassembled, rather than randomly distributed in their membrane-bound state. It is therefore proposed that intra- and intersubunit interactions between segments derived from the core region of the K^+ channel are important for the organization and stabilization of the tetrameric protein in the membrane to form a functional K^+ channel. Also, as is known for water-soluble proteins, interactions between different segments and subunits of the K^+ channel protein may be involved in the intermediate steps of the protein's folding from the secondary structure to the folded, functional channel.

REFERENCES

Baidin, G., & Huang, J. R. (1990) *FEBS Lett. 259*, 254–256.
Bartlett, G. R. (1959) *J. Biol. Chem. 234*, 466–468.
Ben-Efraim, I., Bach, D., & Shai, Y. (1993) *Biochemistry 32*, 2371–2377.
Beschiaschvili, G., & Seelig, J. (1990) *Biochemistry 29*, 52–58.
Bonifacino, J. S., Suzuki, C. K., & Klausner, R. D. (1990a) *Science 247*, 79–82.
Bonifacino, J. S., Cosson, P., & Klausner, R. D. (1990b) *Cell 63*, 503–513.
Bormann, B. J., Knowles, W. J., & Marchesi, V. T. (1989) *J. Biol. Chem. 264*, 4033–4037.
Catterall, W. A. (1988) *Science 242*, 50–61.
Chen, Y. H., Yang, J. T., & Chau, K. H. (1974) *Biochemistry 13*, 3350–3359.
Chung, L. A., Lear, J. D., & DeGrado, W. F. (1992) *Biochemistry 31*, 6608–6616.
Durell, S. R., & Guy, H. R. (1992) *Biophys. J. 62*, 238–250.
Dyson, H. J., Merutka, G., Waltho, J. P., Lerner, R. A., & Wright, P. E. (1992) *J. Mol. Biol. 226*, 795–817.
Frachet, P., Duperray, A., Delachanal, E., & Marguerie, G. (1992) *Biochemistry 31*, 2408–2415.
Frey, S., & Tamm, L. K. (1990) *Biochem. J. 272*, 713–719.
Fung, B. K.-K., & Stryer, L. (1978) *Biochemistry 17*, 5241–5248.
Gazit, E., & Shai, Y. (1993a) *Biochemistry 32*, 3429–3436.
Gazit, E., & Shai, Y. (1993b) *Biochemistry 32*, 12363–12371.
Guy, H. R., & Conti, F. (1990) *Trends Neurosci. 13*, 201–206.
Harris, R. W., Sims, P. J., & Tweten, R. K. (1991) *J. Biol. Chem. 266*, 6936–6941.
Hartmann, H. A., Kirsch, G. E., Drewe, J. A., Taglialatela, M., Joho, R. H., & Brown, A. M. (1991) *Science 251*, 942–944.
Heginbotham, L., & MacKinnon, R. (1992) *Neuron 8*, 483–491.
Hille, B. (1992) *Ionic channels of excitable membranes*, Sinauer, Sunderland, MA.
Jaenicke, R. (1991) *Biochemistry 30*, 3147–3161.
Kahn, T. W., & Engelman, D. M. (1992) *Biochemistry 31*, 6144–6151.
Kenner, R., & Aboderin, A. (1971) *Biochemistry 10*, 4433–4440.
Kirsch, G. E., Drewe, J. A., Hartmann, H. A., Taglialatela, M., de Biasi, M., Brown, A. M., & Joho, R. H. (1992) *Neuron 8*, 499–505.
Kirsch, G. E., Drewe, J. A., De Biasi, M., Hartmann, H. A., & Brown, A. M. (1993) *J. Biol. Chem. 268*, 13799–13804.
Lakowicz, J. R. (1983) *Principles of Fluorescence Spectroscopy*, Plenum, New York.
Lemas, M. V., Takeyasu, K., & Fambrough, D. M. (1992) *J. Biol. Chem. 267*, 20987–20991.
Lemmon, M. A., Flanagan, J. M., Hunt, J. F., Adair, B. D., Bormann, B. J., Dempsey, C. E., & Engelman, D. M. (1992) *J. Biol. Chem. 267*, 7683–7689.
Lemmon, M. A., & Engelman, D. M. (1992) *Curr. Opin. Struct. Biol. 2*, 511–518.
Li, M., Jan, Y. N., & Jan, L. Y. (1992) *Science 257*, 1225–1230.
Liman, E. R., Tytgat, J., & Hess, P. (1992) *Neuron 9*, 861–871.
Lynch, B. A., & Koshland, D. E., Jr. (1991) *Proc. Natl. Acad. Sci. U.S.A. 88*, 10402–10406.
MacKinnon, R. (1991) *Nature 350*, 232–235.
MacKinnon, R., & Miller, C. (1989) *Science 245*, 1382–1385.
MacKinnon, R., & Yellen, G. (1990) *Science 250*, 276–279.
MacKinnon, R., Heginbotham, L., & Abramson, T. (1990) *Neuron 5*, 767–771.
Manolios, N., Bonifacino, J. S., & Klausner, R. D. (1990) *Science 249*, 274–277.
McCormack, K., Lin J. W., Iverson, L. E., & Rudy, B. (1990) *Biochem. Biophys. Res. Commun. 171*, 1361–1371.
McKnight, C. J., Rafalski, M., & Gierasch, M. (1991) *Biochemistry 30*, 6241–6246.
Merrifield, R. B., Vizioli, L. D., & Boman, H. G. (1982) *Biochemistry 21*, 5020–5031.
Papahadjopoulos, D., & Miller, N. (1967) *Biochim. Biophys. Acta 135*, 624–638.
Peled, H., & Shai, Y. (1993) *Biochemistry 32*, 7879–7885.
Pouny, Y., & Shai, Y. (1992) *Biochemistry 31*, 9482–9490.
Pouny, Y., Rapaport, D., Mor, A., Nicolas, P., & Shai, Y. (1993) *Biochemistry 31*, 12416–12423.
Rajarathnam, K., Hochman, J., Schindler, M., & Ferguson-Miller, S. (1989) *Biochemistry 28*, 3168–3176.
Rapaport, D., & Shai, Y. (1991) *J. Biol. Chem. 266*, 23769–23775.
Rapaport, D., & Shai, Y. (1992) *J Biol Chem. 267*, 6502–6509.
Rizzo, V., Stankowsky, S., & Schwarz, G. (1987) *Biochemistry 26*, 2751–2759.
Sahin-Toth, M., Dunten, R. L., Gonzalez, A., & Kaback, H. R. (1992) *Proc. Natl. Acad. Sci. U.S.A. 89*, 10547–10551.
Shai, Y., Bach, D., & Yanovsky, A. (1990) *J. Biol. Chem. 265*, 20202–20209.
Schiffer, M., & Edmondson, A. B. (1967) *Biophys. J. 7*, 121–135.
Schwarz, G., Stankowski, S., & Rizzo, V. (1986) *Biochim. Biophys. Acta 861*, 141–151.
Schwarz, G., Gerke, H., Rizzo, V., & Stankowski, S. (1987) *Biophys. J. 52*, 685–692.
Shen, N. V., Chen, X., Boyer, M. M., & Pfaffinger, P. J. (1993) *Neuron 11*, 67–76.
Shin, H. C., Merutka, G., Waltho, J. P., Wright, P. E., & Dyson, H. J. (1993) *Biochemistry 32*, 6348–6355.
Stankowski, S., & Schwarz, G. (1990) *Biochim. Biophys. Acta 1025*, 164–172.
Sternberg, M. J. E., & Gullick, W. J. (1990) *Protein Eng. 3*, 245–248.
Surewicz, W. K., & Epand, R. M. (1984) *Biochemistry 23*, 6072–6077.
Thiaudière, E., Siffert, O., Talbot, J. C., Bolard, J., Alouf, J. E., & Dufourcq, J. (1991) *Eur. J. Biochem. 195*, 203–213.
Verrall, S., & Hall, Z. W. (1992) *Cell 68*, 23–31.
Wu, C. S. C., Ikeda, K., & Yang, J. T. (1981) *Biochemistry 20*, 566–570.
Yellen, G., Jurman, M. E., Abramson, T., & MacKinnon, R. (1991) *Science 251*, 939–942.
Yool, A. J., & Schwarz, T. L. (1991) *Nature 349*, 700–704.
Yu, X. M., & Hall, Z. W. (1991) *Nature 352*, 64–67.